

## **Synthesis and Plasmonic Properties of Monodisperse Au-Ag Alloy Nanoparticles of Different Compositions from a Single-Source Organometallic Precursor.**

Julian Crespo,<sup>a</sup> Andrea Falqui,<sup>b,c</sup> Jorge García-Barrasa,<sup>a</sup> José M. López-de-Luzuriaga,<sup>a</sup> Miguel Monge,<sup>\*,a</sup> M. Elena Olmos,<sup>a</sup> María Rodríguez-Castillo,<sup>d</sup> Matteo Sestu,<sup>c</sup> Katerina Soulantica<sup>\*,d</sup>

ELECTRONIC SUPPLEMENTARY INFORMATION

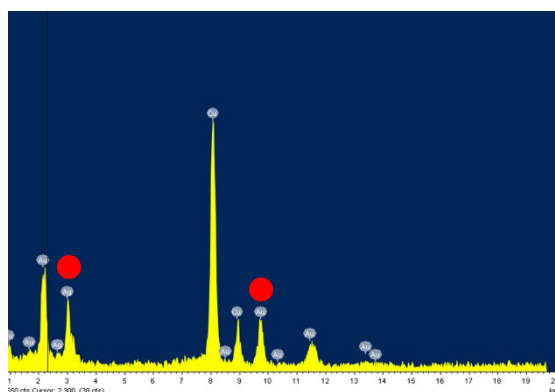
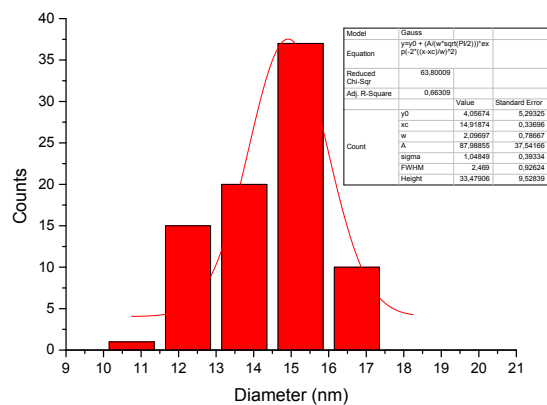


Fig S1: Size distribution (up) and EDS spectrum (bottom) for Au-Ag NPs 1.

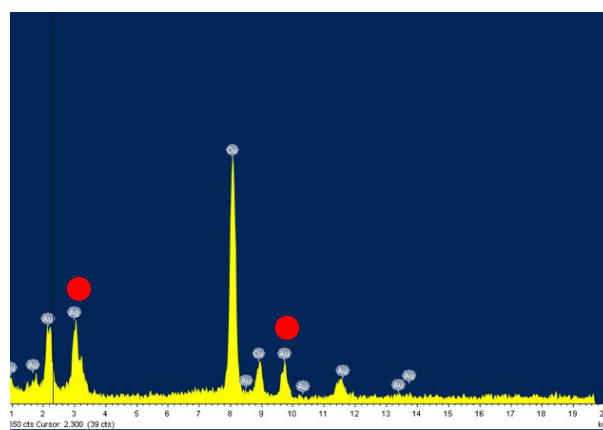
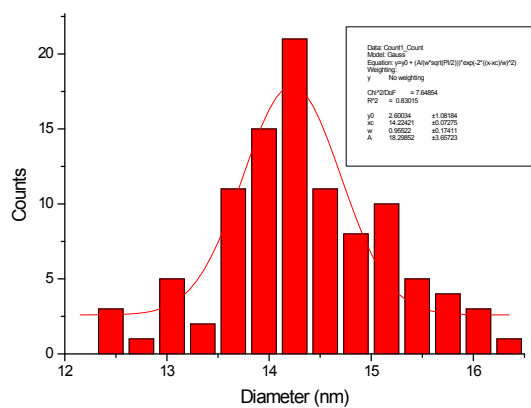


Figure S2. Size distribution (up) and EDS spectrum (bottom) for Au-Ag NPs 2.

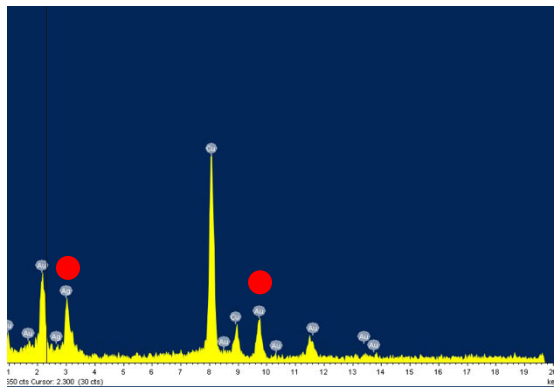
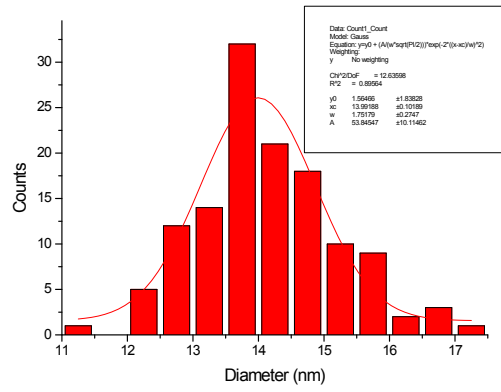


Figure S3. Size distribution (up) and EDS spectrum (bottom) for Au-Ag NPs 3.

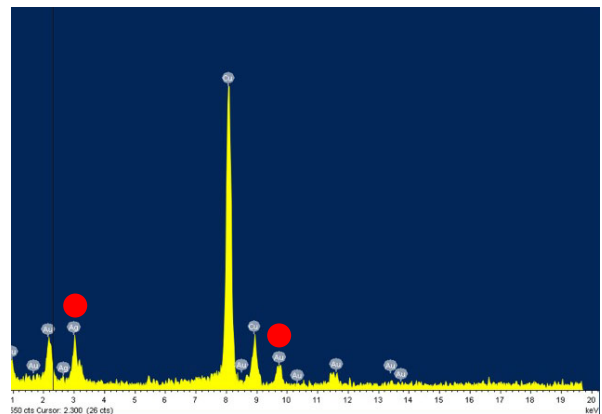
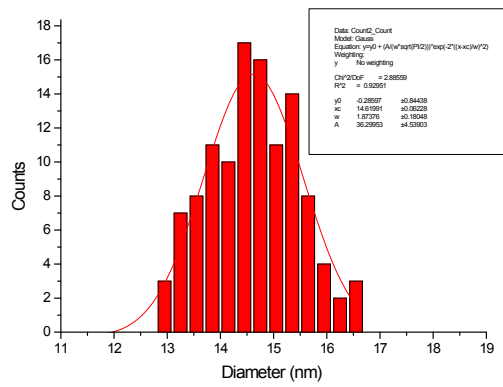


Figure S4. Size distribution (up) and EDS spectrum (bottom) for Au-Ag NPs 4.

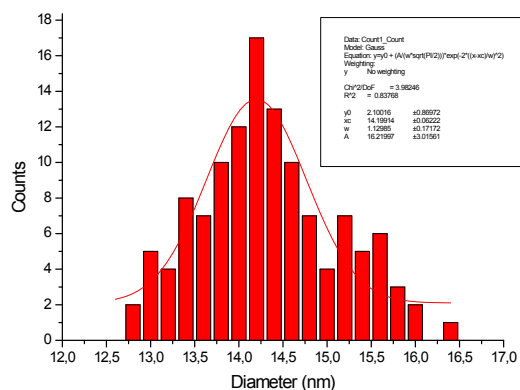


Figure S5. Size distribution for Au-Ag NPs 5.

Table S1. EDS data taken under Bright Field STEM geometry for Au and Ag quantification in Au-Ag NPs 5: areas of the Ag-L $\alpha$  and Au-L $\alpha$ , with correction from the k factors.

spectrum	Ag [%]	Au [%]	Err [%]
P4 (single np)	53	47	4
P7 (single np)	58	42	5
P8 (single np)	61	39	6
P6 (two nps)	54	46	6
P5 (three nps)	56	44	3
P3 (several nps)	57	43	2

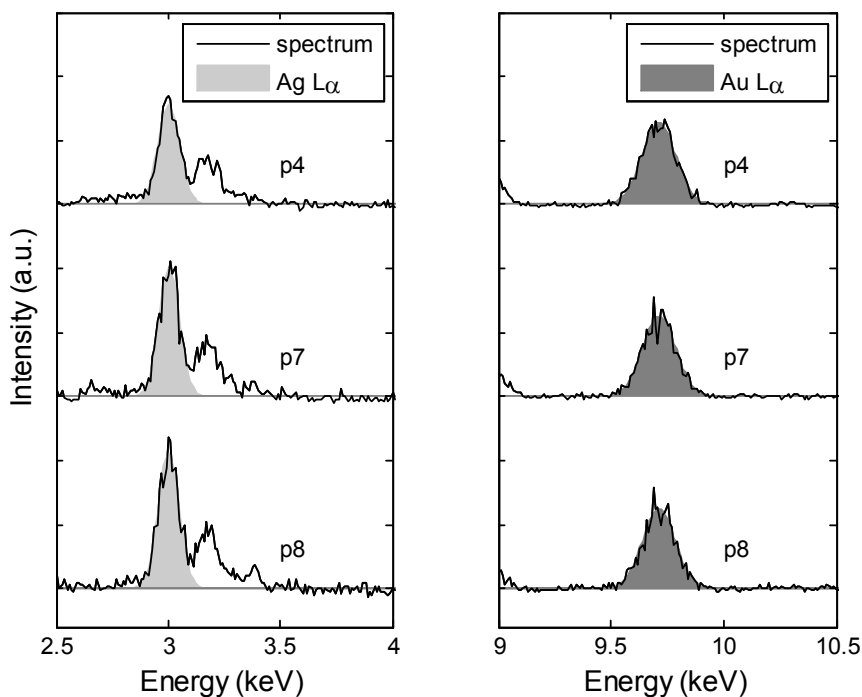


Figure S6. EDS spectra for single nanoparticles Au-Ag NPs (5) taken under Bright Field STEM geometry.

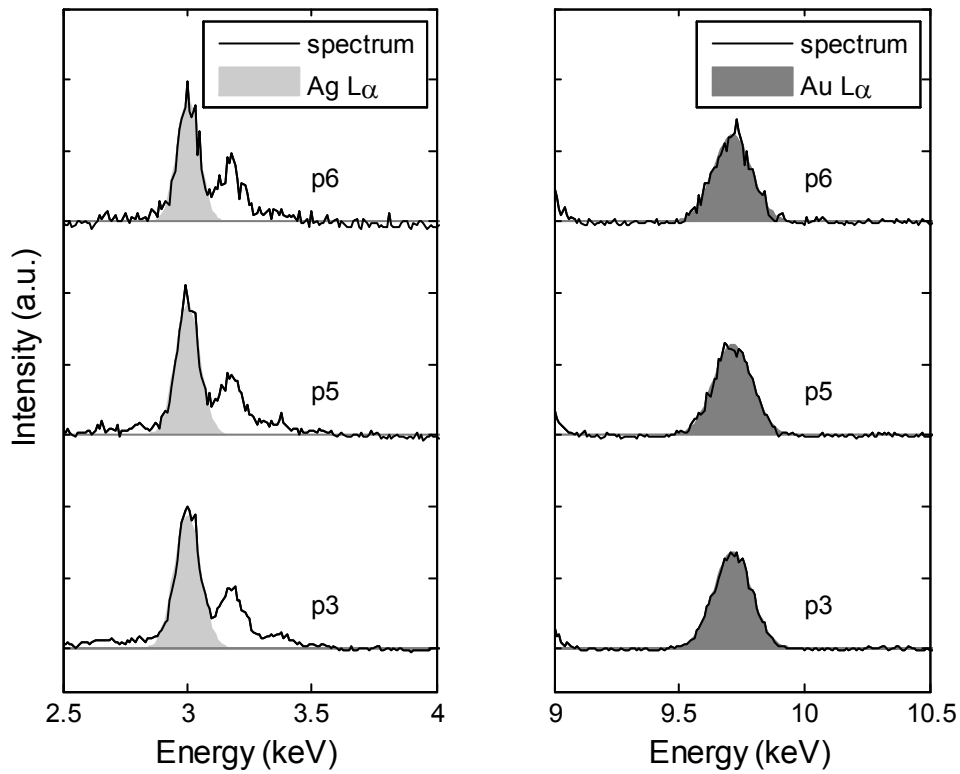


Figure S7. EDS spectra for several nanoparticles Au-Ag NPs (5) taken under Bright Field STEM geometry. Spectrum named P3, taken on several tenths of particles, can be considered as a good estimate of the mean composition

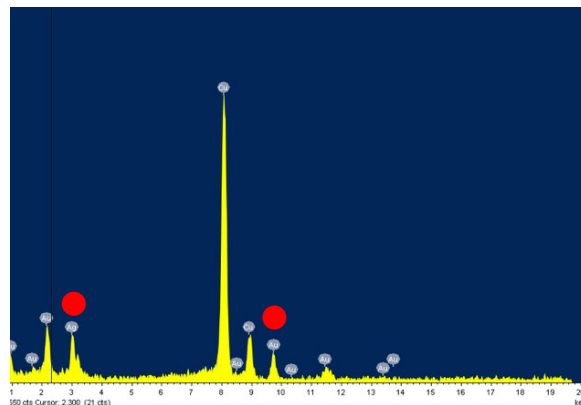
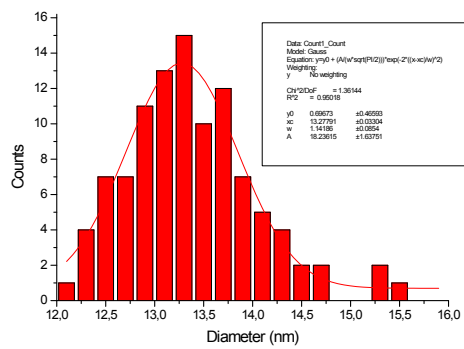


Figure S8. Size distribution (up) and EDS spectrum (bottom) for Au-Ag NPs 6.

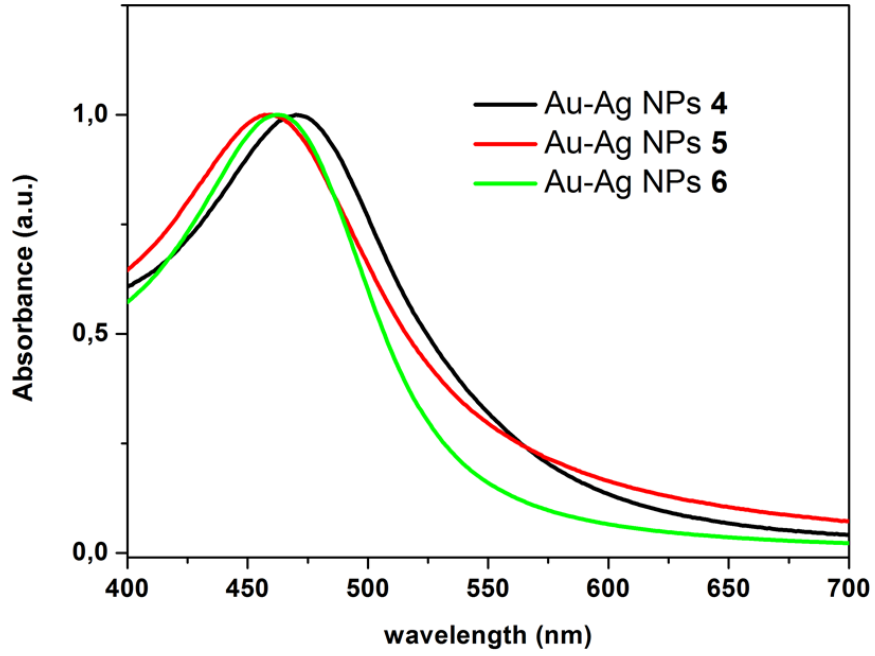


Figure S9. UV/vis spectra for Au-Ag NPs 4-b.

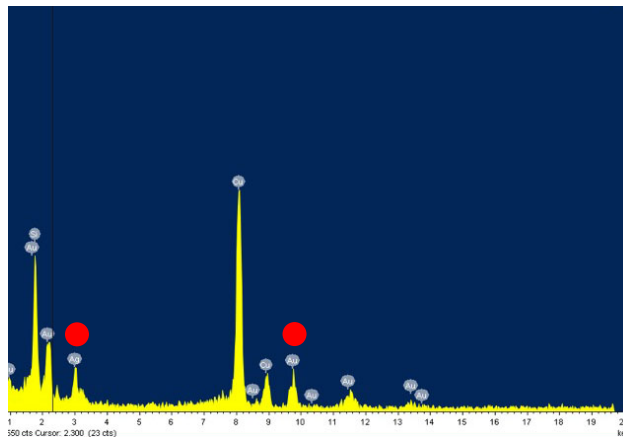
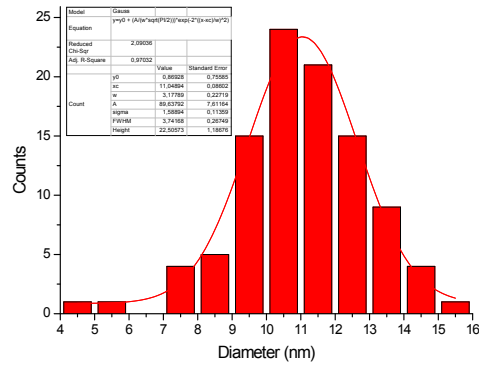


Figure S10. Size distribution (up) and EDS spectrum (bottom) for Au-Ag NPs 7.

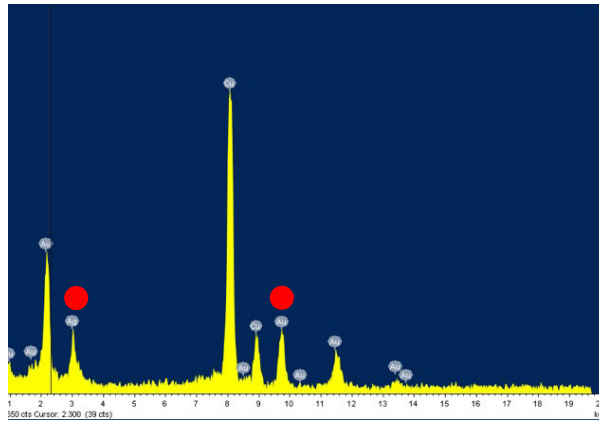
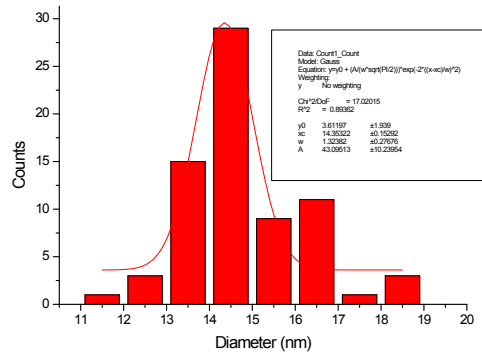


Figure S11. Size distribution (up) and EDS spectrum (bottom) for Au-Ag NPs 8.

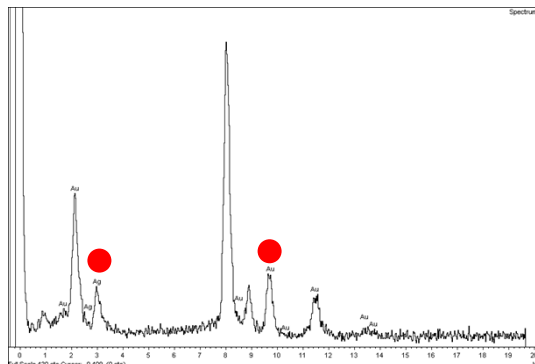
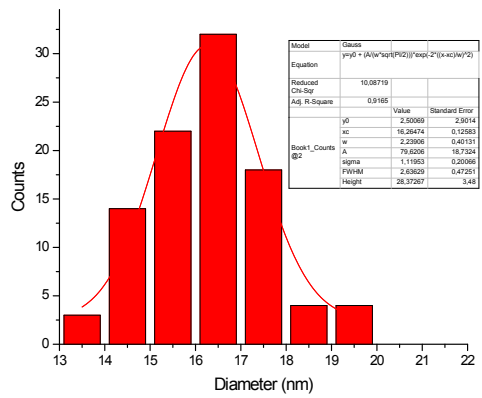


Figure S12. Size distribution (up) and EDS spectrum (bottom) for Au-Ag NPs 9.

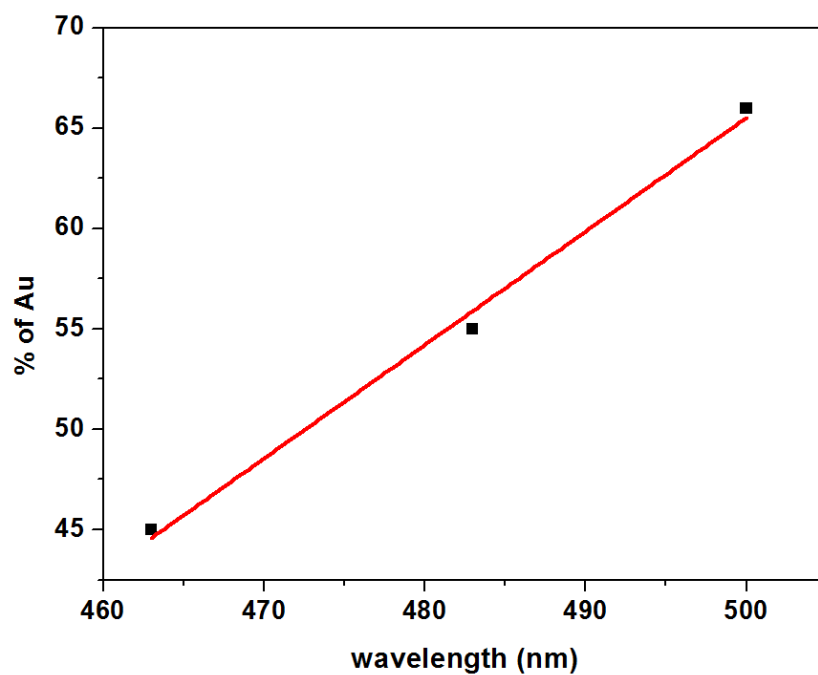


Figure S13. Linear fit displaying the red-shift of the LSPR band (nm) of Au-Ag alloy NPs with increasing Au content ( $r = 0.99$ ).

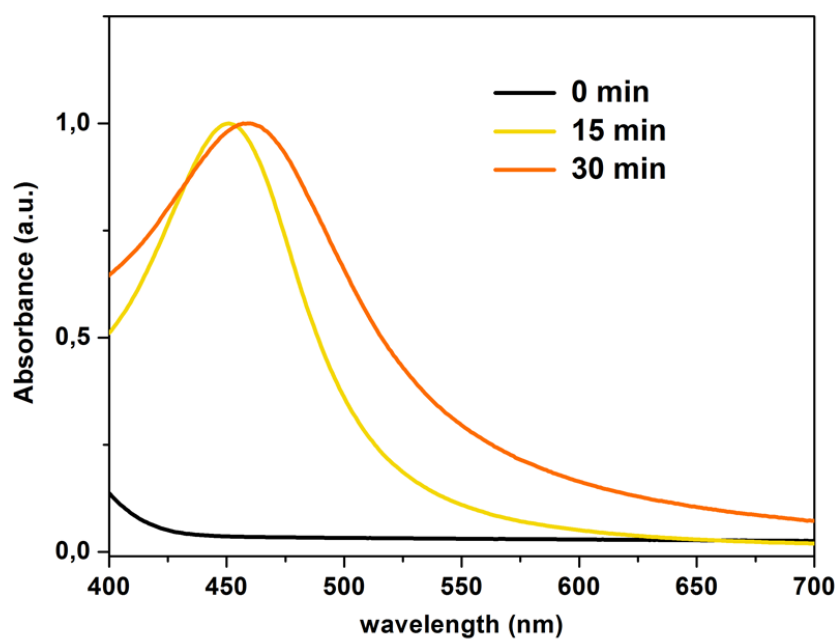




Figure S14. Time-resolved UV/Vis spectra for Au-Ag nanoparticles 5.

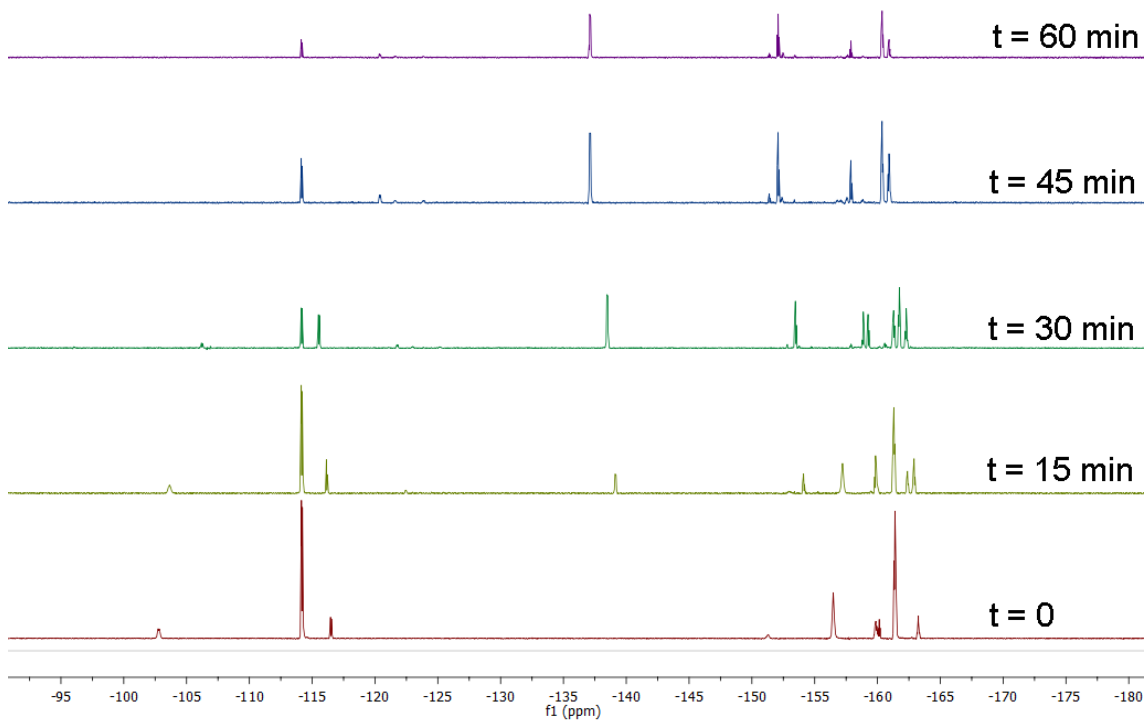


Figure S15: Time-resolved  $^{19}\text{F}$  NMR spectra of the decomposition of complex  $[\text{Au}_2\text{Ag}_2(\text{C}_6\text{F}_5)_2(\text{OEt}_2)]_n$  in the presence of 2 equivalents of Hexadecylamine, in toluene under  $\text{H}_2$

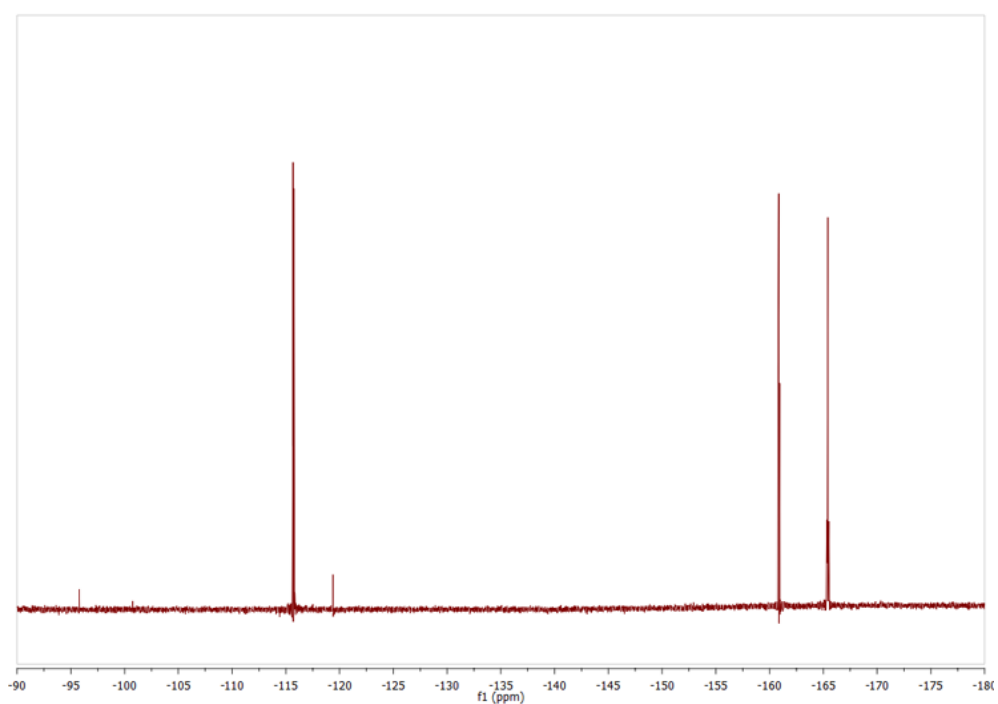


Figure S16.  $^{19}\text{F}$  NMR spectrum for complex  $[\text{Au}_2\text{Ag}_2(\text{C}_6\text{F}_5)_4(\text{OEt}_2)_2]$  in  $d_8$ -Toluene.

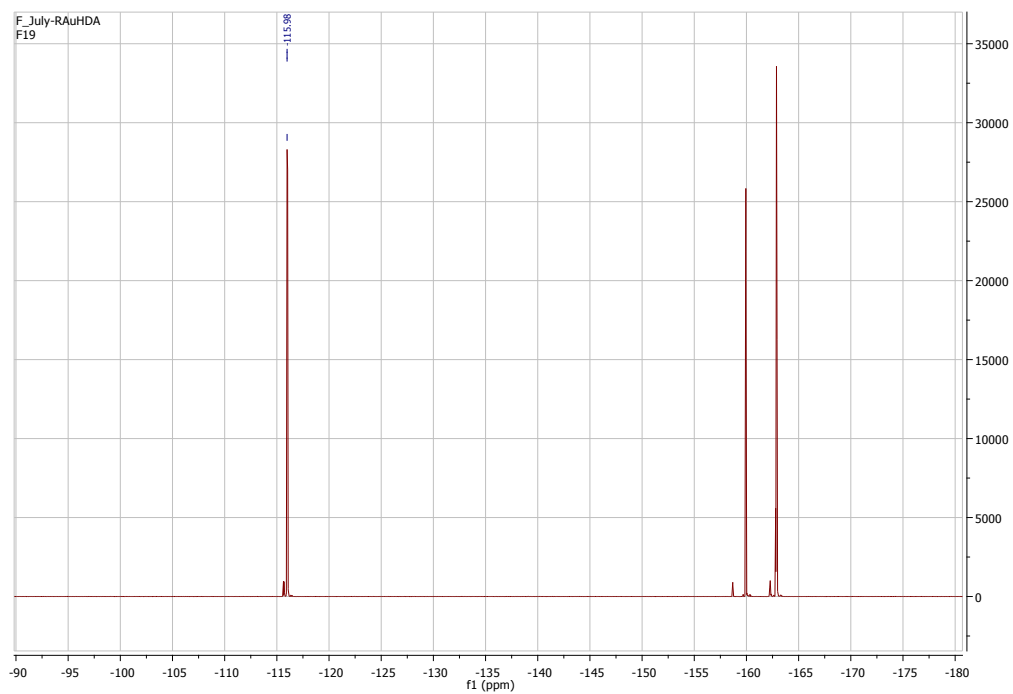


Figure S17.  $^{19}\text{F}$  NMR spectrum for complex  $[\text{Au}(\text{C}_6\text{F}_5)(\text{HDA})]$  in  $d_8$ -Toluene.

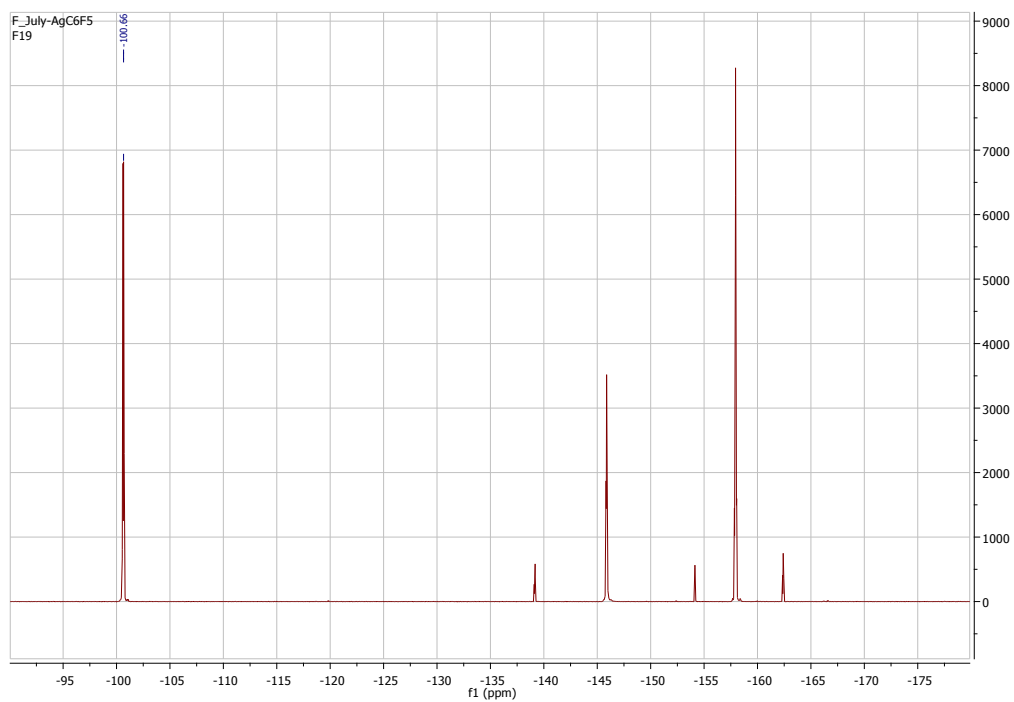


Figure S18.  $^{19}\text{F}$  NMR spectrum for complex  $[\text{Ag}(\text{C}_6\text{F}_5)_n]$  in  $d_8$ -Toluene. The less intense signals correspond to decafluorobiphenyl formed in situ.

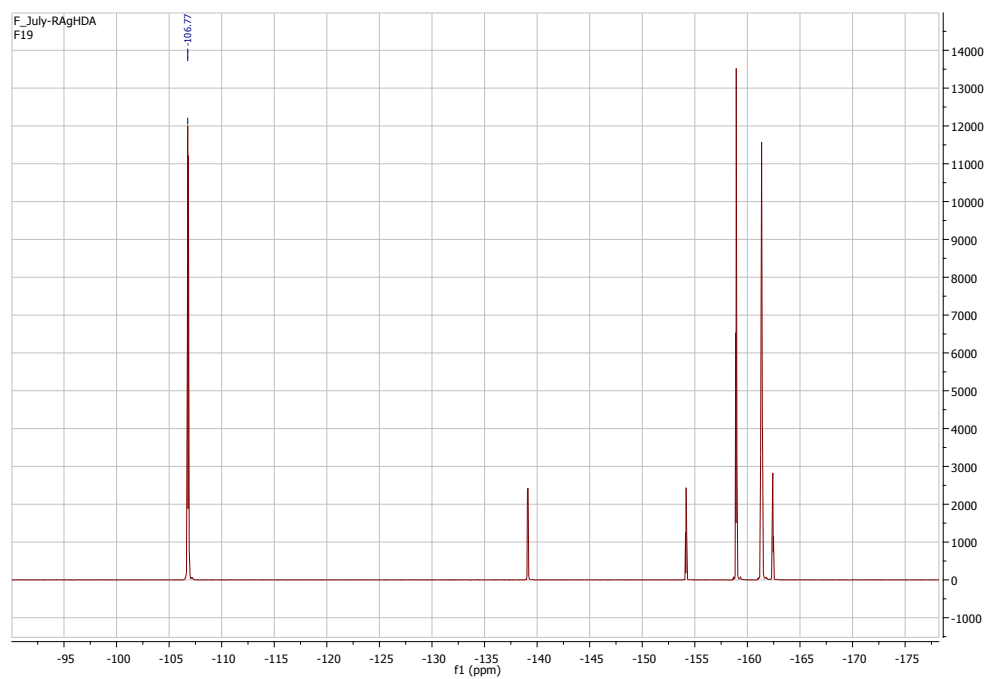


Figure S19.  $^{19}\text{F}$  NMR spectrum for complex  $[\text{Ag}(\text{C}_6\text{F}_5)(\text{HDA})]$  in  $d_8$ -Toluene. The less intense signals correspond to decafluorobiphenyl formed in situ.